Wavelet analysis of pressure fluctuation signals in a gas-solid fluidized bed [*]

ZHEN Ling(甄　玲)[1]，WANG Xiao-ping(王晓萍)[1]，HUANG Hai(黄　海)[1]
CHEN Bo-chuan(陈伯川)[2]，HUANG Chun-yan(黄春燕)[2]

([1] *Instrument Department，Zhejiang University，Hangzhou 310027，China*)

([2] *Chemical Engineering Deptartment，Zhejiang University，Hangzhou 310027，China*)

Received Nov.18，2000；revision accepted Mar.6，2001

Abstract：　It has been shown that much dynamic information is hidden in the pressure fluctuation signals of a gas-solid fluidized bed. Unfortunately，due to the random and capricious nature of this signal，it is hard to realize reliable analysis using traditional signal processing methods such as statistical analysis or spectral analysis，which is done in Fourier domain. Information in different frequency band can be extracted by using wavelet analysis. On the evidence of the composition of the pressure fluctuation signals，energy of low frequency（ELF）is proposed to show the transition of fluidized regimes from bubbling fluidization to turbulent fluidization. Plots are presented to describe the fluidized bed's evolution to help identify the state of different flow regimes and provide a characteristic curve to identify the fluidized status effectively and reliably.

Key words：　wavelet analysis，pressure fluctuation，multi-resolution analysis，fluidized bed，ELF
Document code：　A　　　　**CLC number：**　TQ015.9

INTRODUCTION

Fluidization is assumed to be an efficient means of contacting different particles in various fields such as chemical，metallurgical and pharmaceutical industries. Usually，fluidized bed hydrodynamics are characterized using time-averaged properties，such as the average bubble diameter and rise velocity. Unfortunately，due to their highly random and capricious nature，the pressure fluctuation signals are difficult to investigate and thus is still inadequately modeled，which seriously hampers their industrial applications.

He et al.（1997a）showed the strong non-stationary nature of the pressure fluctuations in a gas-solid fluidized bed，thus showing how no stationary methods can be used to analyze pressure fluctuations in a gas-solid fluidized bed. Furthermore，He et al.（1997b）showed that the pressure fluctuations in a gas-solid fluidized bed could be decomposed into the sum of fractional Brownian motion（FBM）and Gaussian white noise（GWN）caused by gas jetting and the formation of small bubbles near the distributor. Fan et al.（1981）showed that the coalescence and motion of bubbles appear to be the major causes of the pressure fluctuations，while gas jetting，the formation of small bubbles above the distributor，and the raining of fluidized particles in the upper half of the beds，also contribute to the pressure fluctuation.

In this article，the three main components of the pressure fluctuation signals are analyzed by wavelet transform with the help of its multi-resolution character. The original pressure signals can be decomposed at different frequency bands. Then，based on empirical theoretical evidence （He et al，1997b；Fan et al.，1981），we suppose that the energy of the lower frequency band can be used to help us to identify the state of a fluidized bed. Darton et al.（1977）indicated the relationship between the bubbling frequency and gas velocity. Their model gives an index for selecting the frequency band of bubbles. Finally，the energy of the bubble phase is worked out and can be used to distinguish the bubbling fluidization from turbulent fluidization.

THEORETICAL BACKGROUND

The wavelet transform is a very useful tool for analysis of non-stationary signals such as seismic signals. Formalization of wavelet theory was actually initiated by work on seismic signals (Grossmann and Morlet, 1984). It has been refined, particularly as it relates to signal processing by Daubechies (1991). The continuous-time wavelet transform (CTWT) of a function $x(t)$ is defined as:

$$W_x(a,b) = \frac{1}{\sqrt{a}}\int_0^\infty x(t)g\left(\frac{t-b}{a}\right)dt \quad (1)$$

$g(t)$ is a window function known as the analyzing wavelet, the dilation parameter a is known as a scale factor, and b is a translation factor. The wavelet is dilated or compressed by the scale factor. Thus, at low scales, high frequency behavior is localized, while at high scales (when the wavelet is stretched out) low frequency features are better resolved. This is of significant benefit when dealing with signals containing features with various frequency characteristics. Another advantage of the wavelet transform is that the analyzing wavelet can be chosen based on the application.

Since the relevant data is discrete-time, the DTWT (Abry et al., 1994) (instead of the CTWT) is used for the wavelet processing in our work. The DTWT is implemented using the subband coding scheme, two stages of which are illustrated in Fig. 1. The boxes represent linear convolution and the circles represent down sampling by a factor of two (removal of every other sample). The original signal is represented by c^0. At each stage of the DTWT there are two outputs, the scaling coefficients:

$$c^{j+1}[n] = \sum_m h[2n-m]c^j[m], \quad (2)$$

and the wavelet coefficients:

$$d^{j+1}[n] = \sum_m g[2n-m]c^j[m]. \quad (3)$$

In Eq. (3), j represents scale number, and is the discrete-time equivalent of the continuous-time scale factor a. The output scaling coefficients become the input to the next stage in the DTWT. The wavelet coefficients, $d^j (j = 1, 2, 3 \ldots J)$ along with c^J (where J equals the total

number of scales) makes up the discrete-time wavelet representation of the signal c^0.
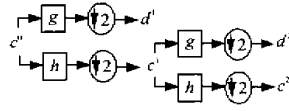

Fig. 1   Two stages(scales) of a wavelet decomposition

The original signal is labeled as c^0. The boxes represent convolution with either g or h. The circles represent down sampling by a factor of two. The outputs, d^j, $(j = 1, 2, \cdots, J)$ are known as the wavelet coefficients. This process can be repeated for the number of scales desired. The circles with upward arrows represent up sampling by a factor of two, which means that a zero is inserted between each sample. The sequences, g and h represent highpass and lowpass filters, respectively. In terms of the DTWT, g is known as the wavelet filter and h is the scaling filter.

Returning to the diagram of Fig. 1, it can be noticed that there are down sampling steps, which result in the length of d^{j+1} being less than the length of d^j. Since our algorithm involves inter-scale comparisons, the wavelet coefficients are interpolated so that the output at each scale contains the same number of points as the original signal. This interpolation is accomplished using up sampling and convolution with a combination of reconstruction filters. The result is a set of coefficients that are interpolated versions of d^j. This type of decomposition is sometimes called multi-resolution analysis (Mallat, 1989).

EXPERIMENT STUDIES

The facilities and procedure employed in our experiments are discussed below.

Facilities

A diagram of the experimental facilities is shown in Fig. 2. The fluidized-bed is associated with a bed column, a distributor and a plenum chamber. The bed is 0.250 m in diameter and 5 m in height. The characteristics of the FCC particles and polyethylene (PE) particles can be found in Table 1.
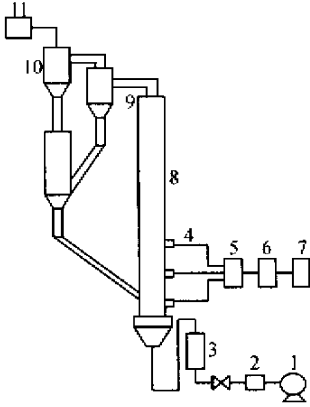
Fig.2   Experimental system
1.fan; 2.cushion pot; 3.rotameter; 4.pressure probes;
5.pressure transducers; 6.A/D board; 7.computer;
8.fluidized bed; 9.first vortex separator; 10.second
vortex separator; 11.hop-pocket

Table 1   Solids characteristics of FCC and PE particles

Characteristics	FCC	PE
Particle density（kg/m^3）	1480	962
Average particle size（μm）	85	280
Minimum fluidization velocity（m/s）	0.0013	0.02
Superficial velocity at which turbulence begins（m/s）	0.668	1.01

The fluidizing gas was air. The holes on the distributor were 2 mm in diameter and had a fractional open area of 3%. Pressure probes were installed on the wall of the bed column at three different heights. The outside opening of each pressure probe was connected to one of the two input channels of a differential pressure transducer producing an output voltage proportional to the pressure difference between the two channels. The remaining channel was exposed to the atmosphere. The working capacity of the transducer was ±5 kPa，and the relative accuracy error was ±0.5%. The sensitivity of the measuring system was 1 V/kPa.

Procedure

The range of experiment conditions is listed in Table 2. For each run of the experiment，the pressure fluctuation signals were detected and subsequently transferred to the main computer through an analog/digital（A/D）board. The sampling frequency was 200 Hz and data length in the same operating condition was 60 000 points.

Table 2   Experimental cperating conditions

Experimental variables	Test range
Superficial gas velocity（m/s）	0.0011
Ratio of static bed height to bed diameter，H_s/D_s	2.0－3.4
Distance above distributor（m）	0.17－0.77

RESULTS AND DISCUSSIONS

The dynamic regime of a fluidized bed mainly depends on the type of particles，the superficial gas velocity，the bed height（or total mass of particles），and the bed diameter. Here，we mainly analyze the superficial gas velocity. Generally speaking，fluidized beds can be operated in six different regimes: particulate fluidization（Group A powders of the Geldart classification only），bubbling fluidization，slugging fluidization（small vessels only），turbulent fluidization，fast fluidization and pneumatic conveying. In this paper，bubbling and turbulent fluidization are discussed.

The voltage-time signals corresponding to the pressure-time signals were collected for a period of time at three different superficial gas velocities.
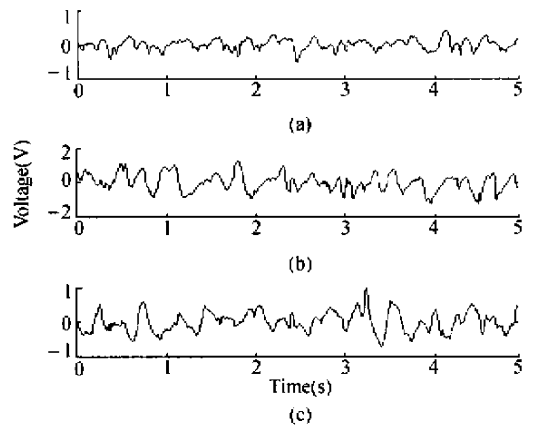

Fig.3   Original signals sampled by pressure transducers at different gas velocity
（a）0.090 m/s；（b）0.362 m/s；（c）0.645 m/s

The corresponding gas flow rates for Fig.3（a），（b），（c）were 0.090 m/s，0.362 m/s，and 0.645 m/s respectively and other operation conditions were unchanged. In fact，with the increase of gas velocity，the operation regimes of

fluidized beds changed accordingly. Different flow regimes can not be easily identified from the original pressure fluctuation plots. The pressure fluctuation signals are mainly generated by the coalescence and motion of bubbles, gas jetting above the distributor and the raining of fluidized particles (Fan et al., 1981). The jetting and the formation of the small bubbles near the distributor are important GWN sources of pressure fluctuation signal, although they may not be the only ones, the GWN is superimposed on the largest pressure fluctuation represented by FBM (He et al., 1997b). In fact, we may safely say that what really reflects the fluidized status between bubbling fluidization and turbulent fluidization is the signal generated by the bubbles phase. It is the disturbance of white noise and vibration of fluidized particles that impeded identification of the fluidized characteristic.

Hence we suppose that the energy of the low frequency band should help us to analyze the fluidized status effectively. With a new plot using this parameter, the energy of the low frequency band (ELF) can give a more reliant and vivid representation. Thanks to the multi- resolution property of the wavelet transform, the original signal can be decomposed at different frequency band. As mentioned above, the wavelet coefficients d^j ($j = 1, 2, 3, \cdots J$) along with c^J, (where J equals the total number of scales) make up the discrete-time wavelet representation of the signal c^0. The sample frequency was 200 Hz. From the property of the wavelet transform, we could learn that d^1 ranged from 100 to 200 Hz, d^2 from 50 to 100 Hz, d^3 from 25 to 50 Hz, d^4 from 12.5 to 25 Hz, d^5 from 6.25 to 12.5 Hz and c^5 from 0 to 6.25 Hz. Darton et al. (1977) indicated the relationship between

the bubbling frequency and superficial gas velocity (SGV), so we chose 5 scales to decompose the signals after the estimation of the bubble frequency according to this model. The wavelet coefficients d^j ($j = 1, 2, 3, 4, 5$) along with c^5 are shown in Fig.4.
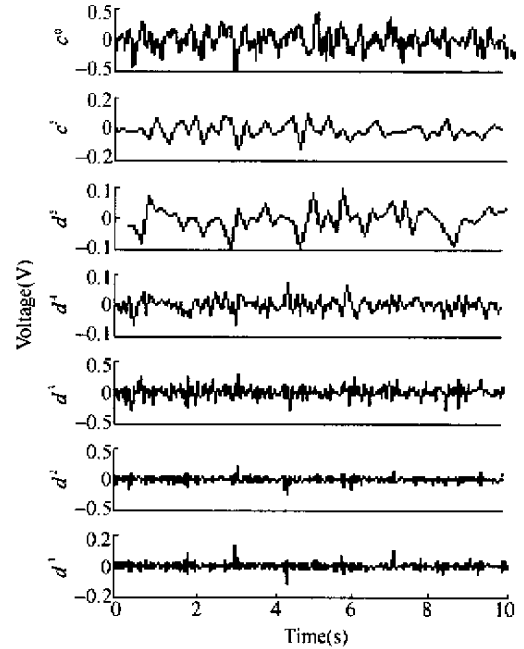

Fig.4   Original signals decomposed at different frequency band

The square sum of wavelet coefficients (V^2) denotes the energy of signal and the square sum of c^5 denotes the energy of the 0 to 6.25 Hz low frequency band (ELF), the energy of which will increase and then decrease with the change of superficial gas velocity (SGV). Finally, we draw the diagram of ELF-SGV. See Fig.5, 6, 7. The regimes of the fluidized bed can be divid-
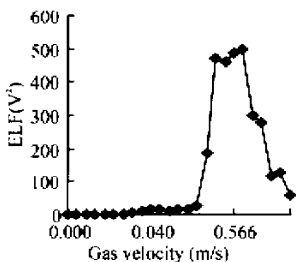

Fig.5   Static bed height 610 mm probe height 470 mm
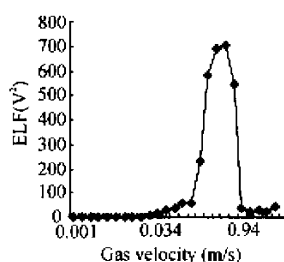

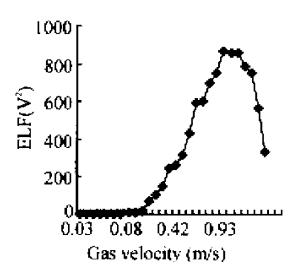Fig.6   Static bed height 830 mm probe height 770 mm

Fig.7   Static bed height 500 mm probe height 320 mm

ed into three sections: particulate fluidization, bubbling fluidization, and turbulent fluidization. There is one tuning points in each plot where the ELF decrease with the increase of gas velocity. We know that the pressure fluctuation is a result of slow and fast propagating pressure waves that move upwards and downwards (Schaaf et al., 1998). Upward moving compression waves originate from the formation and coalescence of gas bubbles, and downward moving compression waves are caused by gas bubble eruptions at the fluidized bed surface. At the very beginning, the ELF is low because there are still few bubbles. When the gas velocity is increased, bubbles are formed and then more bubbles appear. With the increase of the gas velocity, the bubbles are enlarged so much that they begin to break up. When bubble breaking exceeds bubble formation, the regimes begin to change from bubbling fluidization to turbulent fluidization. So the ELF curve is related with the transition. This trend is vividly shown in Fig.8.
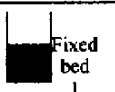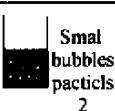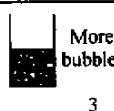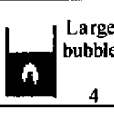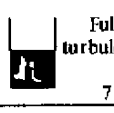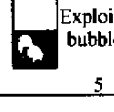

Static beds	Bubbling beds	Turbulent beds
Fixed bed 1		
Smal bubbles pacticls 2	More bubbles 3	Intermediate turbulence 6
	Large bubbles 4	Full turbulence 7
	Exploing bubbles 5	

Fig.8   General view of the change of regimes

CONCLUSIONS

Wavelet analysis provides us an effective tool for analyzing pressure fluctuation signals in a gas-solid bed. We can filter the white noise and disturbance of particle vibration and get the bubble phase signals thanks to the multi-resolution of Wavelet analysis. The parameter ELF gives us a characteristic curve, which can be considered as a good approach to distinguish bubbling fluidization from turbulent fluidization.

References

Abry , P., Flandrin, P., 1994. On the Initialization of the Discrete wavelet transform algorithm, *IEEE Signal Processing Lett.*, **1**:32 − 34.

Darton, R., Lanauze, R. D., Davidson, J. F., et al., 1997. Bubble trowth eue to coalescence in fluidized beds. *Trans. IChemE.*, **55**: 274 − 280.

Daubechies, I., 1991. Time-frequency localization and signal processing. *IEEE Trans. Inform. Theory*, **36**:961 − 1005.

Fan, L.T., Hiraoka, T.H.S., Walawender, W.P., 1981. Pressure fluctuations in a fluidized bed. *AICHE J.*, **27** (3):388 − 396.

Grossmann and Morlet, 1984. Decomposition of Hardy function into square interable wavelets of constant shape. *SIAM J. Math. Anal.*, **15**(4): 723 − 736.

He, Z., Zhang, D.M., Chen, B.C., et al., 1997a. Pressure-fluctuation analysis of a gas-solid fluidized bed using the wigner distribution. *AICHE. J.* **43**(2): 345 − 356.

He, Z., Zhang, W.D., He, K.M., et al., 1997b. Modeling pressure fluctuation via correlation structure in a gas-solids fluidized bed. *AICHE. J.*, **43**(7): 1914 − 1920.

Mallat, 1989. A theory of multiresolution signal decomposition: the wavelet representation. *IEEE Trans.*, *PAMI.* **11**(7): 674 − 693.

Schaaf, J.C., Schouten, J.C., Bleek, C.M.vanden, 1998. Origin paopagation and attenuation of pressure waves in gas-slid fluidized beds. *Powder Technology*, **95**: 220 − 233.